Clinical Cancer Research

Constitutive IRAK4 Activation Underlies Poor Prognosis and Chemoresistance in Pancreatic Ductal Adenocarcinoma

Daoxiang Zhang[1], Lin Li[1], Hongmei Jiang[1], Brett L. Knolhoff[1], Albert C. Lockhart[1], Andrea Wang-Gillam[1], David G. DeNardo[1], Marianna B. Ruzinova[2], and Kian-Huat Lim[1]

Abstract

Purpose: Aberrant activation of the NF-κB transcription factors underlies the aggressive behavior and poor outcome of pancreatic ductal adenocarcinoma (PDAC). However, clinically effective and safe NF-κB inhibitors are not yet available. Because NF-κB transcription factors can be activated by the interleukin-1 receptor-associated kinases (IRAKs) downstream of the Toll-like receptors (TLRs), but has not been explored in PDAC, we sought to investigate the role of IRAKs in the pathobiology of PDAC.

Experimental Design: We examined the phosphorylation status of IRAK4 (p-IRAK4), the master regulator of TLR signaling, in PDAC cell lines, in surgical samples and commercial tissue microarray. We then performed functional studies using small-molecule IRAK1/4 inhibitor, RNA-interference, and CRISPR/Cas9n techniques to delineate the role of IRAK4 in NF-κB activity, chemoresistance, cytokine production, and growth of PDAC cells *in vitro* and *in vivo*.

Results: p-IRAK4 staining was detectable in the majority of PDAC lines and about 60% of human PDAC samples. The presence of p-IRAK4 strongly correlated with phospho-NF-κB/p65 staining in PDAC samples and is predictive of postoperative relapse and poor overall survival. Inhibition of IRAK4 potently reduced NF-κB activity, anchorage-independent growth, chemoresistance, and secretion of proinflammatory cytokines from PDAC cells. Both pharmacologic suppression and genetic ablation of IRAK4 greatly abolished PDAC growth in mice and augmented the therapeutic effect of gemcitabine by promoting apoptosis, reducing tumor cell proliferation and tumor fibrosis.

Conclusions: Our data established IRAK4 as a novel therapeutic target for PDAC treatment. Development of potent IRAK4 inhibitors is needed for clinical testing. *Clin Cancer Res; 23(7); 1748–59. ©2016 AACR.*

Downloaded from http://aacrjournals.org/clincancerres/article-pdf/23/7/1748/2043674/1748.pdf by guest on 26 August 2022

Introduction

To date, the prognosis of pancreatic ductal adenocarcinoma (PDAC) remains dismal with an overall 5-year survival rate of about 8%, which has not changed in the last 4 decades (1, 2). In addition to the universal presence of strong oncogenic events, such as activating mutation of *KRas*, the constitutive activation of the NF-κB transcription factors is another major mechanism that drives the aggressive behavior of PDAC (3–6). Understanding how NF-κB is activated in PDAC is clinically important and has been an area of intense interest (5). For instance, expression of oncogenic KRas upregulates IL1α and GSK3α production to activate the NF-κB pathway in a feedforward manner (7, 8). High miR-301a level suppresses translation of NF-κB–repressing factor protein, thereby activating NF-κB, which in turn enhances miR-301a expression to create a positive feedforward loop (9). However, direct inhibitors of NF-κB or miRNAs have yet to be successful in clinic, indicating the need to explore other strategies to curb this pathway.

Another element that contributes to the recalcitrant nature of PDAC, in addition to its strong intrinsic survival signaling, is the uniquely inflamed and immunosuppressive extrinsic microenvironment, which is believed to hamper cytotoxic T-lymphocyte infiltration and drug delivery (10, 11). In normal tissue, inflammation is triggered by the engagement of the Toll-like receptors (TLR), which activate the innate immune response through the NF-κB and p38/MAPK signaling cascades (12). Several lines of evidence indicate that stimulation of the TLRs could drive NF-κB activity in PDAC. For instance, ligation of TLR4 enhances the invasiveness of PDAC cells in an NF-κB–dependent manner (13). In genetically engineered mouse models, ligation of TLR7 or TLR9 accelerates stromal inflammation and progression of PDAC activation of the NF-κB and MAPK pathways (14, 15). However, the intrinsic role of TLR signaling in neoplastic PDAC cells and how it affects the extrinsic tumor microenvironment have not been thoroughly described.

In this study, we demonstrate for the first time that the interleukin-1 receptor-associated kinase 4 (IRAK4), the master kinase that relays signaling downstream of TLRs (16, 17), is constitutively activated in PDAC cell lines, patient-derived cell lines, and tumor samples. Activated IRAK4 staining positively correlates with activated NF-κB in human PDAC samples, and importantly, portends high postoperative relapse and poor patient survival. We showed that pharmacologic blockade or silencing of IRAK4

[1]Division of Oncology, Department of Internal Medicine, Washington University School of Medicine, Saint Louis, Missouri. [2]Department of Pathology and Immunology, Washington University School of Medicine, Saint Louis, Missouri.

Note: Supplementary data for this article are available at Clinical Cancer Research Online (http://clincancerres.aacrjournals.org/).

D. Zhang and L. Li contributed equally to this article.

Corresponding Author: Kian-Huat Lim, Washington University School of Medicine, 660 South Euclid Avenue, Saint Louis, MO 63110. Phone: 314-362-6157; Fax: 314-362-7086; E-mail: kian-huat.lim@wustl.edu

doi: 10.1158/1078-0432.CCR-16-1121

©2016 American Association for Cancer Research.

Translational Relevance

Activation of the NF-κB transcription factors is a major mechanism that underlies the aggressive behavior of pancreatic ductal adenocarcinoma (PDAC). However, effective and safe inhibitor of the NF-κB is not available, underscoring a need to curb this pathway by alternative means. We now present the first evidence that activation of the interleukin-1 receptor-associated kinase 4 (IRAK4) is a major driving mechanism of NF-κB activity in PDAC. The presence of phospho-IRAK4 staining in PDAC samples is associated with poor patient prognosis. Pharmacologic inhibition or silencing of IRAK4 significantly thwarted tumorigenic growth of PDAC cells and augmented the killing effect of chemotherapy. Therefore, our data provide preclinical rationale for the development of IRAK4 inhibitors as a new class of targeted agent for clinical testing in combination with chemotherapy, and indicate phospho-IRAK staining as a potential biomarker for patient selection and pharmacodynamics studies in future clinical trials involving IRAK4 inhibitor.

potently suppressed NF-κB activity, abolished the tumorigenic potential of human and murine PDAC cells, and greatly sensitized PDAC cells to various chemotherapeutics *in vivo* and *in vitro*. Our data lay a solid foundation for testing IRAK4 inhibitors as a novel class of therapeutic agents for PDAC treatment.

Materials and Methods

PDAC lines

Human PDAC lines AsPC-1, BxPC-3, Capan-1, Capan-2, CFPAC-1, HPAF-II, HPAC, MIA Paca-2, PANC-1, SW1990, and HPNE cells were purchased from the ATCC, which performs authentication on its own cell lines. All cells were used for fewer than 6 months after receipt or resuscitation from cryopreservation. HPDE, MPanc96, and Hs766T were kind gifts from Dr. David Linehan (University of Rochester, NY). KRas-Ink4a cells were a kind gift from Dr. David DeNardo (Washington University, MO) and were published (18). Patient-derived PDAC cell lines (PDCL) Pa01c, Pa02c, and Pa14c were kind gifts from Dr. Channing Der (University of North Carolina, NC) and published (19, 20). HPNE and HPDE cells are immortalized, normal human pancreatic epithelial cells.

Cancer-associated fibroblasts

Human cancer-associated fibroblasts (CAFs) were isolated from the PDAC specimen of a patient who underwent the Whipple procedure and expanded using a published method (21). CAFs were confirmed to be α-SMA–positive and pan-cytokeratin–negative by immunofluorescence (IF).

Human PDAC samples, tissue microarray, and survival analysis

FFPE PDAC and matched adjacent normal pancreatic tissues diagnosed between years 2000 and 2010 were retrieved from the Department of Pathology and Immunology at Washington University, MO, under Institutional Review Board–approved protocol (#201404143). All selected patients had documented follow-up to 6 years after surgery. None received neoadjuvant treatment prior to surgery, but all received adjuvant treatment containing either 5-fluorouracil (5-FU) or gemcitabine. Pancreatic tissue array (catalog # PA961B) was purchased from US Biomax.

Immunohistochemistry and immunofluorescence

Immunohistochemistry (IHC) was performed using p-IRAK4 (T345S; A8A8; ABNOVA; 1:200), p-NF-κB/p65 (S536; Abcam ab86299; 1:200), and p-TAK1 (S184/187; Bioss bs-3439R; 1:200). IHC scores were determined by the sum of intensity (0: none, 1: faint, 2: weak, 3: moderate, 4: strong) and distribution (0: none, 1: <25%, 2: 25%–50%, 3: 50%–75%, 4: >75%) sub-scores. All samples were scored two times in a blinded manner. Further details were provided in Supplementary Data.

Plasmids and creation of stable cell lines

Stable knockdowns were generated using pSuper-Retro-Puro or neo/GFP plasmids encoding scramble sequence, or indicated shRNAs as described (22). Further details included in Supplementary Data.

Drugs and reagents

5-FU, gemcitabine, and paclitaxel were purchased from the Siteman Cancer Center Pharmacy. The IRAK1/4 inhibitor, N-(2-Morpholinylethyl)-2-(3-nitrobenzoylamido)-benzimidazole, was purchased from Sigma (I5409). IMD-0354 was purchased from Selleckchem.

In vitro cell viability assay, synergism analysis, and soft-agar assay

Viability was assayed using Resazurin colorimetric analysis; synergism studies were performed as described (23); soft-agar assay was performed as described (24). Further details were provided in Supplementary Data.

In vitro CAF migration/invasion assay

CAFs were added to rehydrated 8-μm pore, 24-well cell culture inserts (with or without collagen; BD Bioscience). Serum-free conditioned media (200 μL) from PANC-1 or Capan-1 cells were added to lower chambers. After 24 hours, uninvaded CAFs were removed from the upper chamber, and invaded cells were fixed with 4% paraformaldehyde, stained with toluidine blue overnight, and counted under microscope.

Immunoblotting and quantitative real-time PCR

Details were provided in Supplementary Data.

Cytokine array analysis

Human Cytokine Antibody Array C3 (catalog # AAH-CYT-3) was purchased from Raybio. Membranes were incubated with serum-free conditioned media collected from 70% to 80% confluent Capan-1 cells treated with DMSO or 10 μmol/L of IRAK1/4i overnight (about 16 hours) and processed according to the manufacturer's protocol. Identical results were obtained from a repeat experiment using different sets of Capan-1–conditioned media.

NF-κB reporter assay

NF-κB reporter activity was performed using Dual-Glo Luciferase Assay System and read with Synergy *H4* Hybrid Multi-Mode Microplate Reader. All experiments were done three times in triplicate and data represented as mean ± SEM.

Downloaded from http://aacrjournals.org/clincancerres/article-pdf/23/7/1748/2043674/1748.pdf by guest on 26 August 2022

Xenograft tumorigenesis assay and *in vivo* bioluminescence imaging

All animal experiments were conducted according to Institutional Animal Care and Use Committee protocol (#20130191). Details were provided in Supplementary Data.

Statistical analysis

Normal distributions were compared by two-tailed Student *t* test or ANOVA; tumor growth curves were compared using Mann–Whitney *U* tests; survivals were analyzed using Kaplan–Meier method and Log-rank test. Statistical analyses were performed with Graphpad Prism v6.0. *P* values <0.05 were considered as statistically significant.

Results

IRAK4 is constitutively phosphorylated in human PDAC cell lines, surgical samples, and is associated with poor prognosis

To explore the intrinsic role of TLR signaling in PDAC, we first investigated the phosphorylation/activation status of IRAK (25, 26), particularly IRAK1 and IRAK4 in a panel of well-characterized human PDAC lines. We found IRAK1 to be constitutively phosphorylated in 9, and IRAK4 in 11, of 12 lines in the absence of TLR ligand stimulation. In contrast, IRAK4 phosphorylation was barely detected in both, whereas IRAK1 was weakly phosphorylated in one, of two nontransformed pancreatic ductal cell lines, HPNE and HPDE (Fig. 1A). Consistent with published literature, the majority of PDAC lines also showed constitutive phosphorylation of NF-κB/p65 and iκB (5, 6). Similarly, p-IRAK4 is detectable in four early-passaged patient-derived cell lines (PDCLs), along with increased p-NF-κB/p65 and p-iκBα (Supplementary Fig. S1A).

We next investigated the phosphorylation status of IRAK4 (p-IRAK4) in 103 resected human PDAC samples by IHC using a phospho-antibody that was previously reported in melanoma (27). We found p-IRAK4 to be present and significantly stronger in the ductal epithelia of 20 out of 30 (or 66.7%) PDAC samples (Fig. 1B and C), compared with their matched normal pancreatic tissues. In all 103 PDAC samples analyzed, p-IRAK4 expression is present in 58.8% of cases at various intensities and extent in the neoplastic ductal cells (Fig. 1C), which is significantly higher than normal pancreatic tissue ($P = 0.0002$). As a control, total IRAK4 protein is detected in both normal pancreatic and PDAC tissues (Fig. 1B). We next validated this finding using a commercially available pancreatic tissue microarray and found p-IRAK4 IHC staining to be present at various intensities in 63.5% of PDAC samples, which is comparable to our findings in surgical samples (Supplementary Fig. S1B and S1C).

To gain an initial insight of whether p-IRAK4 contributes to NF-κB activity in PDAC, we next determined the correlation between the staining intensities of p-IRAK4 and p-NF-κB/p65. We found complete overlap of p-IRAK4 and p-NF-κB/p65 IHC staining in the neoplastic epithelia of surgical PDAC samples (Fig. 1D). IHC analysis of 85 PDAC samples from tissue microarray showed various degrees of p-NF-κB/p65 staining intensities in 87% of samples (Supplementary Fig. S1B and S1D), and we noted strong correlation between the staining intensities of p-IRAK4 and p-NF-κB/p65 (Spearman *R* 0.87, $P < 0.0001$; Fig. 1E). In a genetically engineered p48-Cre; $p53^{Flox/WT}$;LSL-$KRas^{G12D}$ (or KPC) mouse model of PDAC, both p-IRAK4 and p-NF-κB/p65 stainings are present at a very low level starting from early pancreatic intraepithelial neoplasia (PanIN-1) and become increasingly stronger during progression to higher grade PanIN-2, PanIN-3, and PDAC (Fig. 1F), indicating a potential role of IRAK4 and NF-κB activity during PDAC development.

Because p-IRAK4 staining is detectable in the majority but not all PDAC samples, we determined whether p-IRAK4 staining is associated with prognosis. Remarkably, we found that patients with positive p-IRAK4 PDAC had a significantly higher chance of postsurgical relapse and worse overall survival despite adjuvant treatment, compared with patients with negative p-IRAK4 tumors (6-year median relapse-free survival: 12.56 vs. 32.95 months, log-rank $P = 0.0122$; 6-year median overall survival: not reached vs. 19.05 months, log-rank $P = 0.0065$). We observed no difference in tumor size, nodal status, tumor grade, age, and gender distribution between p-IRAK4–positive versus negative tumor (not shown), establishing IRAK4 activation as an independent prognostic factor in PDAC. Together, our findings conclude that IRAK4 is frequently activated and associated with aggressive behavior of PDAC, and provide a strong rationale to investigate the pathogenic role of IRAK4 in PDAC.

IRAK1/4 drives NF-κB activity and anchorage-independent growth of PDAC cells

To determine whether IRAK4 contributes to NF-κB activity in PDAC cells, we treated PDAC lines with a widely described dual IRAK1/4 inhibitor (28). We found dose-dependent suppression of phosphorylated IRAK1, IRAK4, iκBα, and NF-κB/p65 in all four PDAC lines tested (Fig. 2A). Consistently, IRAK1/4i significantly suppressed NF-κB–driven luciferase activity in five of six PDAC lines, but not in BxPC-3 which has barely detectable p-IRAK1 and p-IRAK4 (Fig. 2B). Furthermore, IRAK1/4i dose-dependently suppressed the anchorage-independent (AI) growth of eight of 10 established PDAC lines in soft agar, and all three PDCLs tested, but had no significant suppression on the viability of HPNE, HPDE, and most PDAC cells in monolayer culture except for mild effect in PANC-1 (Fig. 2C; Supplementary Fig. S2A–S2C). To exclude the nonspecific effect of IRAK1/4i, ectopic expression of a constitutively active IKKβ mutant (S177E/S181E) rendered IRAK1/4i ineffective in suppressing the NF-κB–driven reporter activity and AI growth of PANC-1 cells (Fig. 2D and E). As a complementary experiment, although the NF-κB activity of BxPc-3 line is independent of IRAK1/4 inhibition and can be suppressed by the IKKβ inhibitor IMD-0354, overexpression of wild-type, but not kinase-dead, IRAK4 significantly increased p-NF-κB, AI growth, and rendered BxPC-3 cells sensitive to IRAK1/4i (Fig. 2F and G). These results suggest that the NF-κB activity of PDAC is dependent on IRAK1/4.

To further dissect the individual role of IRAK1 and IRAK4 in NF-κb activation, we performed shRNA knockdown of IRAK1, IRAK4, or both in PDAC lines. Stable knockdown of IRAK1 or IRAK4 by shRNAs, and more so with both, potently inhibits p-IKKα/β and p-NF-κB in human PDAC lines and a murine PDAC cell line (KRas-Ink4a) derived from transgenic *KRas*^{G12D}; *Ink4a*/Arf$^{-/-}$ mice (Fig. 2H; Supplementary Fig. 2D). Interestingly, knockdown of IRAK1 had little effect on p-IRAK4 in two PDAC lines tested (Fig. 2H), suggesting either insufficient IRAK1 knockdown or that IRAK4 is activated independent of IRAK1 in PDAC.

Downloaded from http://aacrjournals.org/clincancerres/article-pdf/23/7/1748/2043674/1748.pdf by guest on 26 August 2022

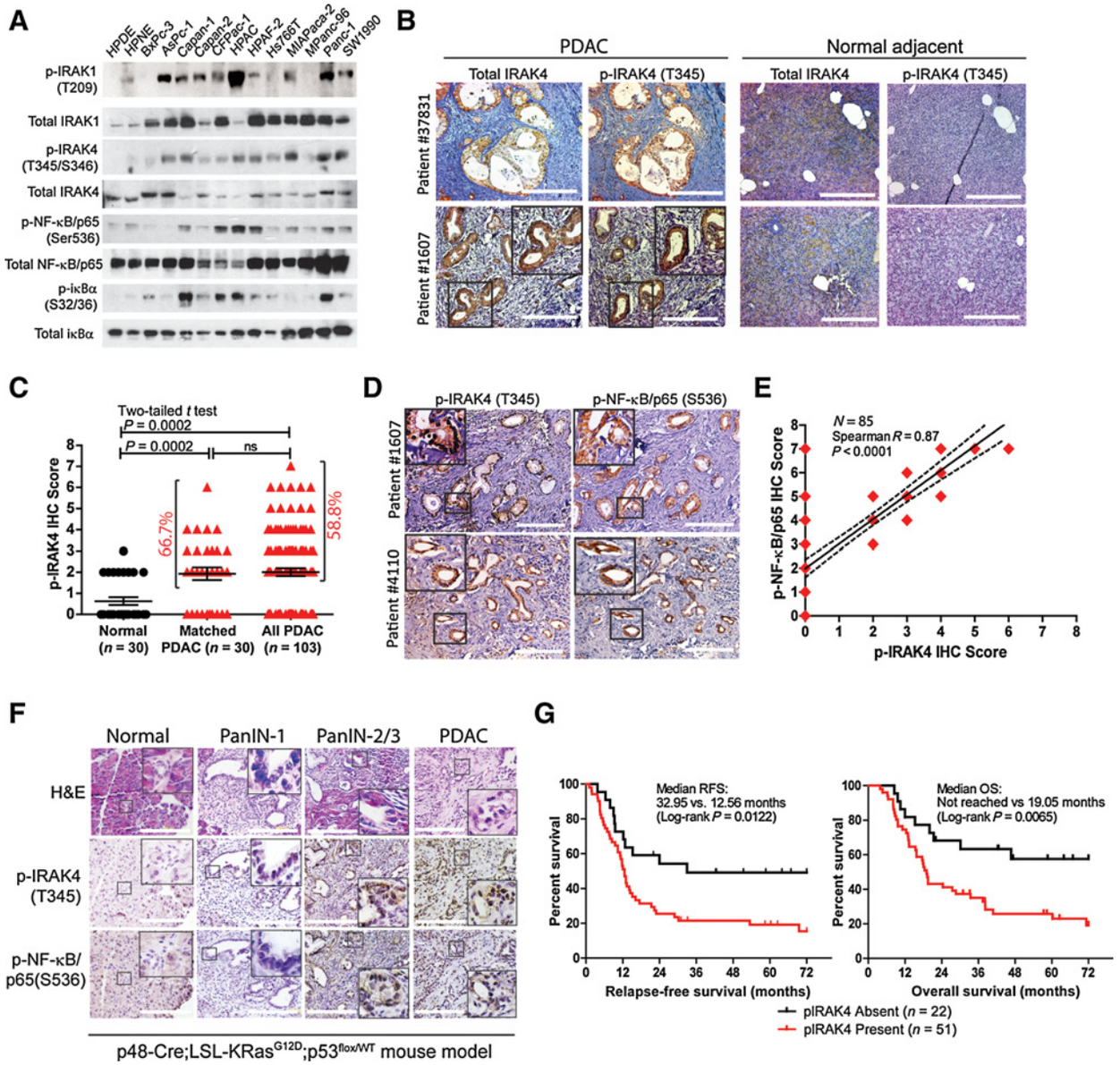

Figure 1.

IRAK4 is constitutively phosphorylated in PDAC cell lines and surgical samples. **A,** Western blots showing phosphorylation status of IRAK1, IRAK4, NF-κB, and iκBα in 12 PDAC lines versus two nontransformed pancreatic ductal lines (HPDE and HPNE). **B,** Representative IHC images showing p-IRAK4 staining in PDAC surgical samples ($N = 103$), but not in the adjacent normal pancreatic tissue, of two patients. Total IRAK4 staining is present in both normal and PDAC tissues (scale bar, 200 μm). **C,** Scatter plot showing quantification of p-IRAK4 IHC score on matched normal and PDAC samples ($N = 30$ each), and all PDAC cases ($N = 103$; ns, not significant). **D,** Representative IHC images showing overlap of p-IRAK4 and p-NF-κB/p65 staining in PDAC tissues of two patients. **E,** Correlation analysis of p-IRAK4 and p-NF-κB/p65 IHC intensity of 85 PDAC samples from tissue microarray. Shown here is best-fit line with 95% confidence interval. **F,** Representative hematoxylin and eosin (H&E) and IHC images of the pancreas of KPC mice during progression from preneoplastic PanIN lesions to PDAC. **G,** Relapse-free survival (RFS) and overall survival (OS) by Kaplan–Meier analysis of patients with PDAC who underwent Whipple resection as stratified by the presence or absence of p-IRAK4 staining ($N = 73$).

Consistent with our findings with IRAK1/4i, knockdown of IRAK4 or both IRAK1 and IRAK4, and less so of IRAK1, reduce AI growth of human and murine PDAC lines (Fig. 2I and J; Supplementary Fig. S2E). In PANC-1 cells, the suppressive effect of shIRAK1+4 on AI growth could be rescued with re-introduction of constitutively-active IKKβ mutant (Supplementary Fig. S2F), again supporting the notion that the IRAKs function predominantly through the IKK-NF-κB cascade in PDAC. Furthermore, genetic ablation of IRAK4 with CRISPR/Cas9n technique significantly reduced AI growth of PANC-1 and a PDCL line, Pa01c (Fig. 2K).

We next performed knockdown-rescue experiments to delineate the requirement of kinase function of IRAK1 and IRAK4 in PDAC cells growth. We found that the decreased soft-agar growth

Downloaded from http://aacrjournals.org/clincancerres/article-pdf/23/7/1748/2043674/1748.pdf by guest on 26 August 2022

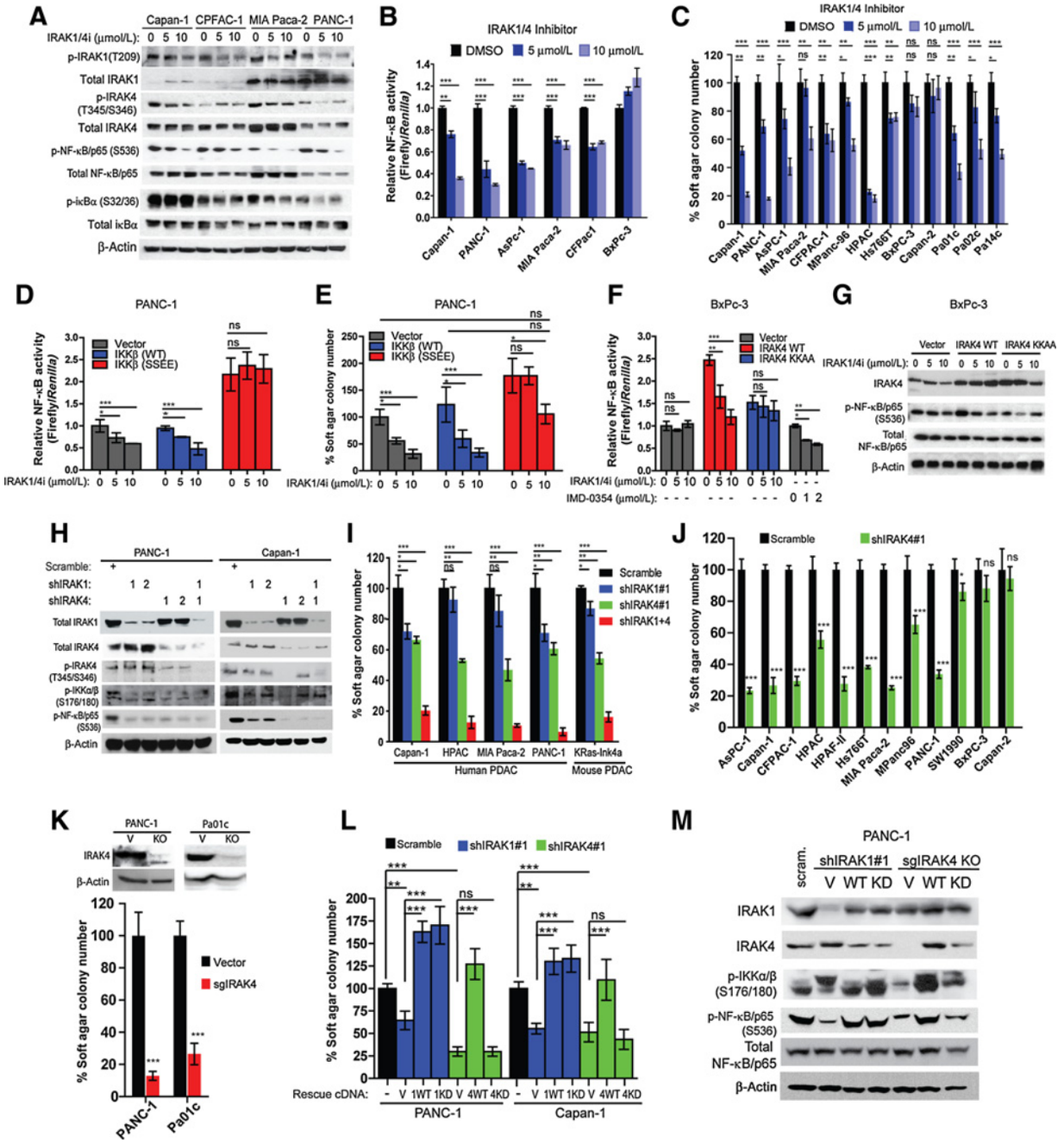

Figure 2.

IRAK4 kinase contributes to NF-κB activity and AI growth of PDAC cells. **A,** Western blots showing suppression of p-IRAK1, p-IRAK4, p-NF-κB/p65, and p-iκBα in the indicated PDAC lines following overnight treatment with IRAK1/4 inhibitor at two different concentrations. **B,** NF-κB luciferase reporter assay showing dose-dependent suppression of relative NF-κB activity (Firefly luciferase activity/Renilla) following overnight treatment of IRAK1/4 inhibitor in six PDAC lines stably expressing NF-κB–driven firefly luciferase and Renilla; mean ± SEM. **C,** AI growth of PDAC lines seeded in DMSO or two different concentrations of IRAK1/4i for 3 to 4 weeks. **D,** Relative NF-κB luciferase reporter activity. **E,** AI growth of PANC-1 cells stably expressing vector, wild-type IKKβ, or constitutively active IKKβ (S177E, S181E) treated with DMSO or two different concentrations of IRAK1/4i overnight. Relative NF-κB reporter activity (**F**) and (**G**) Western blots showing changes in p-NF-κB/p65 of BxPc-3 cells stably expressing vector, wild-type IRAK4, or kinase-dead IRAK4 (K213A, K214A) treated with DMSO or two different concentrations of IRAK1/4i overnight. **H,** Western blots showing changes of p-IKKα/β, p-NF-κB/p65, and p-IRAK4 following stable knockdown of IRAK1, IRAK4, or both in PDAC cell lines. **I,** Effect of IRAK1 or/and IRAK4 knockdown on AI growth of the indicated PDAC lines. **J,** AI growth of PDAC lines stably expressing scramble shRNA or shIRAK4. **K,** AI growth of IRAK4-ablated PANC-1 and Pa01c lines generated by CRISPR/Cas9n technology. **L,** AI growth of Capan-1 and PANC-1 cells stably expressing scramble shRNA, shIRAK1, or shIRAK4 followed by rescue with empty vector, wild-type, or kinase-dead IRAKs. **M,** Western blots showing changes in p-IKKα/β and p-NF-κB/p65 of PANC-1 cells transduced with shRNA against IRAK1 followed by re-expression of vector, wild-type IRAK1, or kinase-dead IRAK1(K239A), or sgRNA against IRAK4 followed by re-expression of vector, wild-type IRAK4, or kinase-dead IRAK4 (K213A or K214A; *, $P < 0.05$; **, $P < 0.01$; ***, $P < 0.001$ by two-tailed t test).

Downloaded from http://aacrjournals.org/clincancerres/article-pdf/23/7/1748/2043674/1748.pdf by guest on 26 August 2022

in shIRAK4-transduced Capan-1 and PANC-1 cells could be rescued by re-introduction of wild-type, but not kinase-dead IRAK4 (KK213AA), whereas the suppressive effect of shIRAK1 could be rescued with both wild-type and kinase-dead IRAK1 (K239A). Supporting this finding and consistent with published reports (29–31), the kinase activity of IRAK4, but not IRAK1, is essential in activating IKKα/β and NF-κb in PANC-1 cells (Fig. 2M). Resonating this observation, we also found that TLR7-induced NF-κB activation in HEK293T cells requires the kinase activity of IRAK4, but not IRAK1 (Supplementary Fig. S2G). Together, our data concluded that IRAK4 kinase activity is essential in driving NF-κb activity in PDAC and should be explored as a therapeutic target.

Suppression of IRAK1/4 induces apoptosis and sensitizes pancreatic cancer cells to chemotherapeutic agents

Activated NF-κB is a major mechanism that underlies chemoresistance in PDAC (5, 6, 32). Because the IRAK kinases drive NF-κB activity in PDAC cells, we next determined whether suppression of IRAK1/4 augments the cytotoxic effect of chemotherapeutics. We found that exposure of Capan-1 and PANC-1 cells to gemcitabine significantly upregulates NF-κB activity, as reported (32). However, such induction could be stifled by IRAK1/4i (Fig. 3A). Mechanistically, knockdown of IRAK1 and/or IRAK4 was sufficient to induce PARP cleavage, an indicator of apoptosis, which was further enhanced by exposure to gemcitabine (Fig. 3B). The chemosensitization effect of shIRAK1+4 could be partially

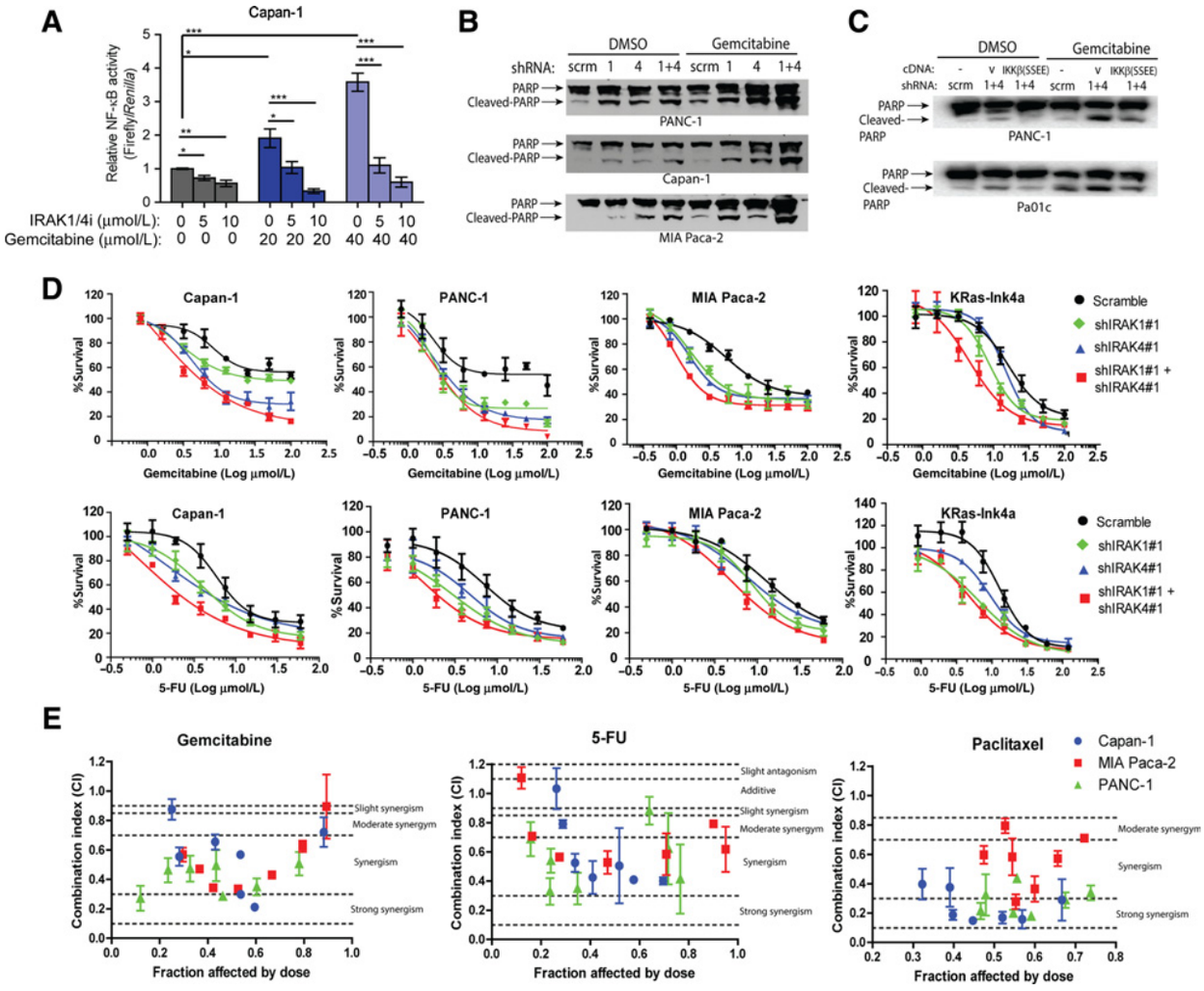

Figure 3.

IRAK1/4 inhibition sensitizes PDAC cells to the cytotoxic effect of chemotherapy *in vitro*. **A,** NF-κB luciferase reporter assay showing suppressive effect of IRAK1/4i in gemcitabine-induced NF-κB activation in Capan-1 cells. **B,** Western blots showing increased PARP cleavage following introduction of shIRAK1, shIRAK4, or both in PDAC lines treated with DMSO or 10 μmol/L of for 48 hours. **C,** Western blots showing partial reversal of gemcitabine-induced PARP cleavage by re-expression of activated IKKβ in shIRAK1+4-expressing PANC-1 and Pa01c cells. **D,** Alamar blue assays showing increased sensitivity of shIRAK1, shIRAK4, or shIRAK1+IRAK4 PDAC cell lines to gemcitabine or 5-FU. Each graph represents one of three independent experiments done in triplicates; mean ± SEM. Change in IC_{50} is provided in Supplementary Table S1. **E,** Median effect analysis showing interaction between IRAK1/4i with chemotherapeutic agents in three different PDAC lines analyzed using Compusyn software. Data represent combined mean ± SEM of three independent experiments each performed in duplicates. Horizontal dotted lines indicate the boundaries for each interaction classification (23).

Downloaded from http://aacrjournals.org/clincancerres/article-pdf/23/7/1748/2043674/1748.pdf by guest on 26 August 2022

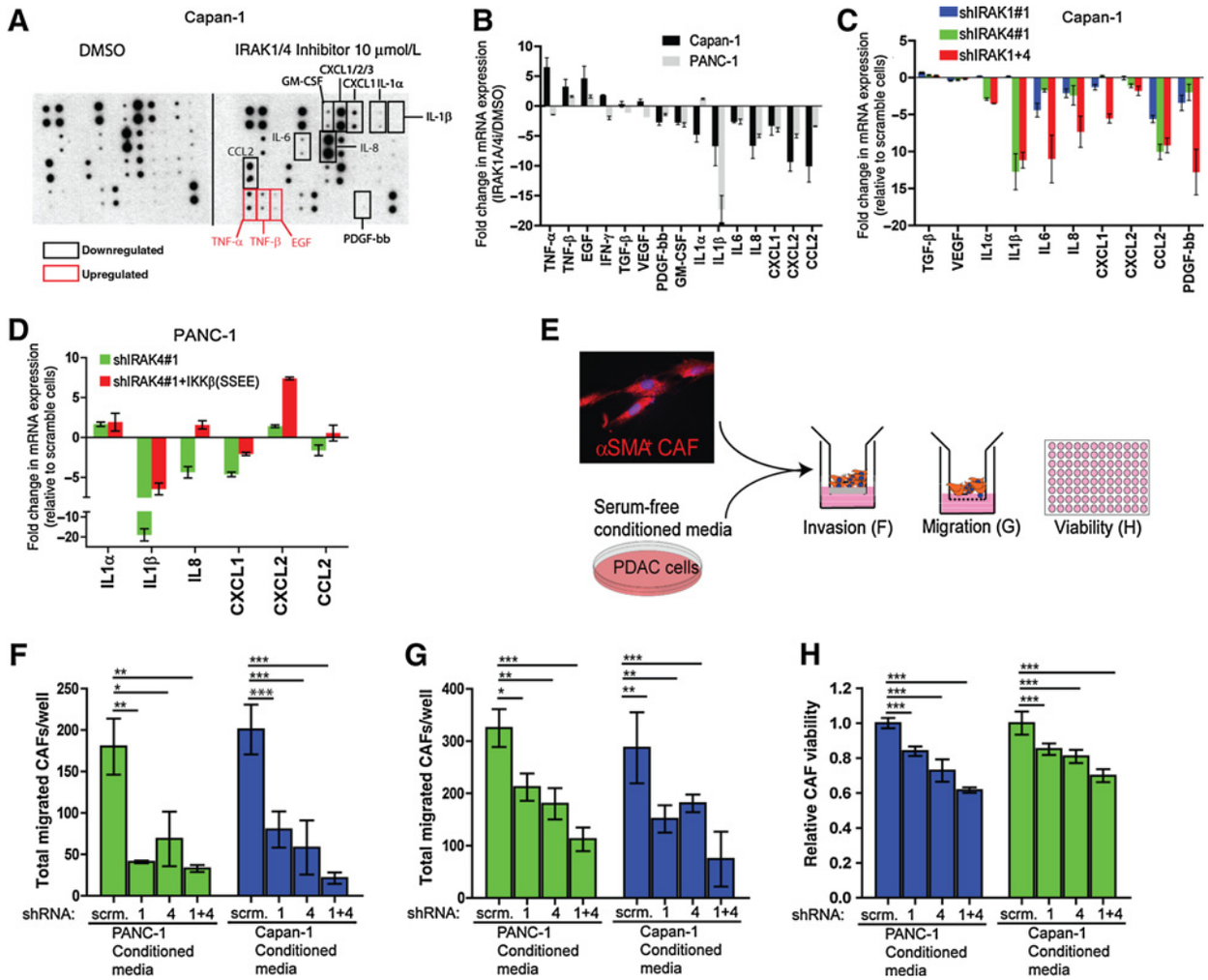

Figure 4.

IRAK1/4 controls secretion of inflammatory chemokines and cytokines from PDAC cells to augment invasion, migration, and viability of CAFs. **A,** Cytokine array showing altered secretion of chemokines/cytokines in serum-free conditioned media collected from Capan-1 cells treated with either DMSO or 10 μmol/L of IRAK1/4 inhibitor overnight. Identical results were obtained from a repeat experiment. **B,** RT-PCR showing fold changes in mRNA levels of the indicated genes in Capan-1 and PANC-1 cells treatment with 10 μmol/L of IRAK1/4 inhibitor relative to DMSO overnight. **C,** RT-PCR showing fold change in mRNA levels of the indicated genes in Capan-1 cells transfected with shRNA against IRAK1 or/and IRAK4, relative to scramble transfected cells. **D,** qRT-PCR showing fold change of the indicated genes in PANC-1 cells transfected with shIRAK4#1 with empty vector or activated IKKβ (SSEE) mutant. All qRT-PCR were done at least twice, each in three biological replicates and three technical triplicates normalized to GAPDH. Final fold changes were compared with either vehicle- or vector-treated cells. Data represent mean ± SEM. **E,** Schematics showing experimental design to elucidate the effect of conditioned media collected from PDAC cells on α−SMA^{+} CAFs. **F–H,** Transwell collagen invasion, migration, and viability by Alamar blue assay of CAFs cultured in serum-free conditioned media collected from Capan-1 or PANC-1 cells stably expressing scramble shRNA, shIRAK1, shIRAK4, or both. Data presented as mean ± SEM. Experiments were done twice in triplicates (*, $P < 0.05$; **, $P < 0.01$; ***, $P < 0.001$ by ANOVA).

rescued by reintroduction of constitutively active IKKβ mutant (Fig. 3C), again supporting IRAK1/4 as therapeutic targets upstream of NF-κB. Consistently, PDAC cells stably expressing shIRAK1 or shIRAK4, and to a much greater extent, both, were significantly more sensitive to the killing effect of gemcitabine and 5-FU, two commonly used chemotherapeutics in PDAC treatment (Fig. 3D), as shown by significant reductions in IC_{50} of both chemotherapeutic agents compared with scramble cells (Supplementary Table S1). To translate these findings, we perform synergism analysis by treating Capan-1, MIA Paca-2 and PANC-1 with combination mixtures of IRAK1/4i plus each chemotherapeutic agent at constant ratios, as described (23). In all three PDAC lines, we observed various degrees of synergism between IRAK1/4i and each chemotherapeutic agent (Fig. 3E). Overall, our findings provide a strong rationale for testing IRAK1/4i plus chemotherapy *in vivo*.

IRAK1/4 drives production of inflammatory cytokines and chemokines that drive migration, invasion, and proliferation of CAFs

Targeting the desmoplastic tumor microenvironment (TME) is emerging as another attractive therapeutic strategy in PDAC. The

Downloaded from http://aacrjournals.org/clincancerres/article-pdf/23/7/1748/2043674/1748.pdf by guest on 26 August 2022

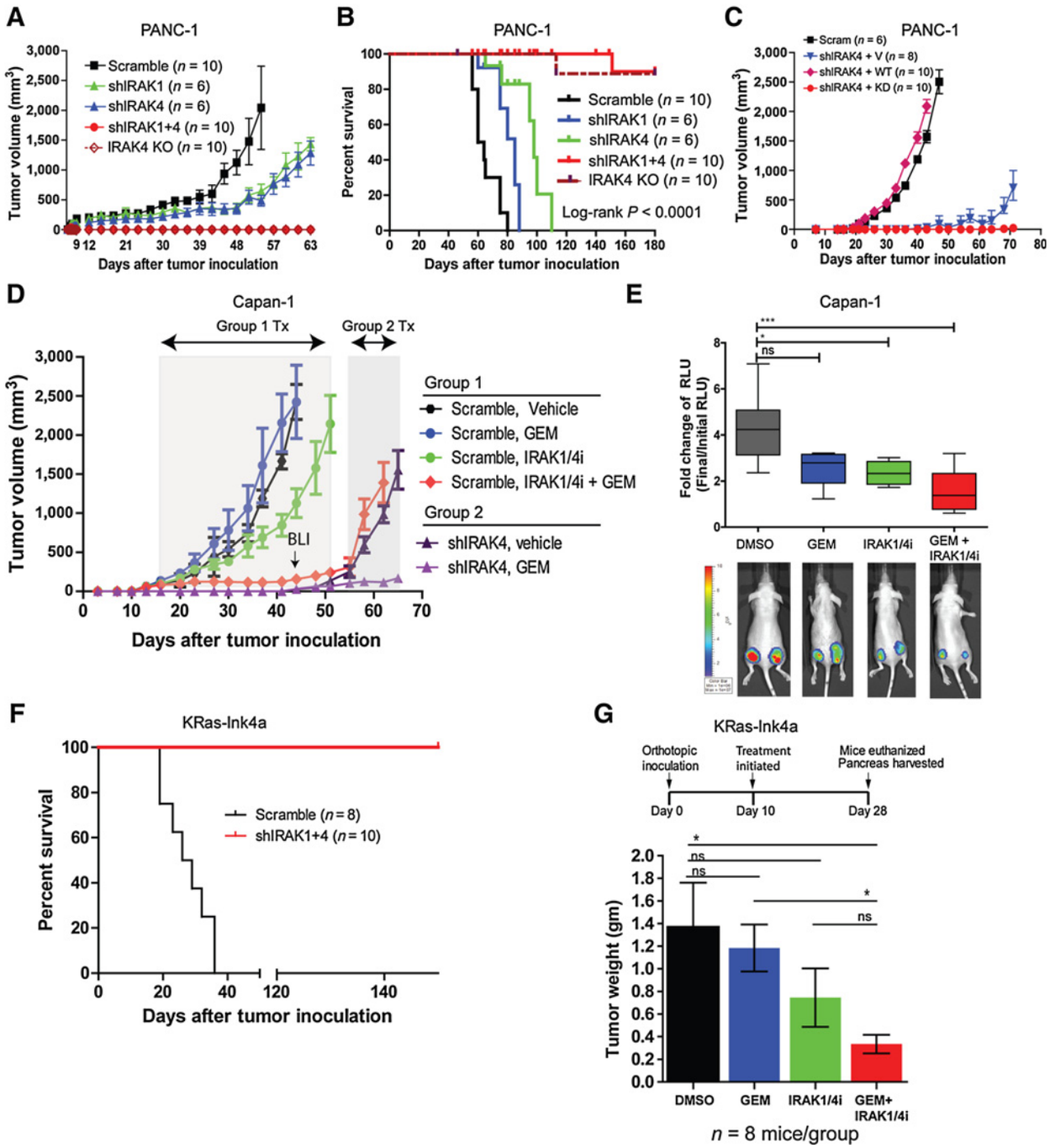

Figure 5.

Genetic or pharmacologic suppression of IRAK4 abrogates PDAC tumorigenesis and augments the therapeutic effect of gemcitabine *in vivo.* Growth kinetics (**A**) and Kaplan-Meier (**B**) curves of PANC-1 cells stably expressing a scramble shRNA, shIRAK1, shIRAK4 or both, or PANC-1 cells with *IRAK4* ablated with by CRISPR/Cas9n, following subcutaneous inoculation in nude mice. **C,** Growth kinetics of PANC-1 cells stably expressing the indicated shRNA and IRAK4 rescue variants following subcutaneous inoculation in nude mice. **D,** Growth kinetics of nude mice inoculated subcutaneously at bilateral flanks with Capan-1/luciferase cells stably expressing scramble shRNA (group 1) or shIRAK4 (group 2), which were then treated as indicated after tumors have achieved a volume of 50 to 100 mm^3 ($N = 5$ mice, 10 tumors/cohort). Bioluminescence imaging (BLI) was performed at 44 days after inoculation when scramble-arm reached maximum allowed volume. **E,** Box plot showing relative fold change of bioluminescence readings (final/initial readings) of Capan-1 tumors treated as indicated at day 44. **F,** Kaplan–Meier survival of FVB/NJ mice orthotopically inoculated with KRas-Ink4a cells stably expressing a scramble shRNA or shIRAK1+shIRAK4. **G,** Final average tumor weights ± SEM from the pancreas of immunocompetent FVB/NJ mice orthotopically inoculated with of KRas-Ink4a cells which were then treated with either DMSO, gemcitabine, IRAK1/4i, or both ($N = 8$/cohort; *, $P < 0.05$; **, $P < 0.01$; ***, $P < 0.001$ by ANOVA).

Downloaded from http://aacrjournals.org/clincancerres/article-pdf/23/7/1748/2043674/1748.pdf by guest on 26 August 2022

highly inflamed and immunosuppressive TME is widely believed to be driven by cytokines and chemokines secreted by PDAC cells (7, 11, 33–35). Because IRAK activation induces cytokine secretion in normal innate immune response, we speculate that production of inflammatory cytokines/chemokines in PDAC is also regulated by IRAK. Indeed, the abundance of IL1α, IL1β, IL8, PDGF, GM-CSF, CCL2, CXCL1, and CXCL2 in the conditioned medium of Capan-1 cells was reduced following IRAK1/4i treatment (Fig. 4A). As controls, secretion of TNFα, TNFβ, and EGF was slightly increased, whereas other factors including TGFβ and VEGF were unchanged following IRAK1/4i treatment. These changes were confirmed by qRT-PCR using Capan-1 cells treated with IRAK1/4i or transduced with IRAK1 or/and IRAK4 shRNAs (Fig. 4B and C). Interestingly, knockdown of IRAK1 had less pronounced effect on the transcription of these factors compared with IRAK4- or double-knockdown cells, suggesting IRAK4 as the predominant driver in cytokine/chemokine production in PDAC (Fig. 4C). As confirmation, we observed very similar, but not identical, changes in production of these secreted factors in another PDAC line, PANC-1 (Fig. 4B). Notably, the suppressive of shIRAK4 on cytokine/chemokine production in PANC-1 could be partially reversed by re-introduction of activated IKKβ mutant (Fig. 3D).

Because many of these affected chemokines/cytokines are known to induce desmoplasia, we next asked whether IRAK1/4 inhibition would impair the ability of PDAC cells to stimulate the growth and behavior of CAFs (Fig. 4E). Indeed, condition media collected from IRAK1, IRAK4, or IRAK1/4 knocked-down Capan-1 and PANC-1 cells were greatly defective in inducing invasion, migration, and proliferation of CAFs (Fig. 4F–H). Based on these results, we speculate that, in addition to curbing the survival of neoplastic PDAC cells, IRAK1/4 inhibition can attenuate the fibrotic TME of PDAC and is an attractive therapeutic strategy.

IRAK4 kinase is essential for pancreatic tumorigenesis *in vivo*

We next tested whether inhibition of IRAK1 and/or IRAK4 can impede PDAC growth *in vivo*. Consistent with our findings in soft agar, knockdown of IRAK1 or IRAK4 significantly thwarted the tumorigenic potential of PANC-1 cells and extended the survival of tumor-bearing mice (Fig. 5A and B). Strikingly, shIRAK1+shIRAK4 or IRAK4-ablated PANC-1 cells completely lost tumorigenic potential *in vivo*, although one mouse from each group died unexpectedly from unknown causes (Fig. 5A and B). Consistent with our previous findings (Fig. 2L), the suppressive effect of shIRAK4 *in vivo* could be rescued by re-expression of wild-type, but not kinase-dead, IRAK4 (Fig. 5C). We next confirmed these findings using another PDAC line, Capan-1, which stably expresses firefly luciferase and either scramble shRNA (group 1) or shIRAK4 (group 2). We chose to focus on IRAK4 because it is now the target of interest. Treatment was started once tumor establishment was confirmed by palpation and positive bioluminescence signal. Group 1 mice were randomized to receive vehicle, gemcitabine, IRAK1/4 inhibitor, or both; whereas group 2 mice were treated with vehicle or gemcitabine. In group 1 mice, combined gemcitabine and IRAK1/4i significantly impeded tumor growth, although IRAK1/4 inhibitor alone showed modest yet statistically significant reduction in tumor growth compared with vehicle (Fig. 5E). Consistently, Capan-1 tumors treated with both gemcitabine and IRAK1/4i, and less so with IRAK1/4i alone, had significantly lower bioluminescence signals compared with vehicle- or gemcitabine-treated tumors (Fig. 5E). Notably, mice in all four cohorts showed no sign of distress or body weight loss during treatment (Supplementary Fig. S3A). Contrary to scramble tumors, shIRAK4 (group 2) tumors could be suppressed by gemcitabine alone (Fig. 5D), resonating previous findings that shIRAK4 sensitizes PDAC cells to gemcitabine *in vitro* (Fig. 3D).

Next, to better mimic the native TME and to understand the consequence of systemic IRAK inhibition in an immunocompetent setting, we resorted to the murine KRas-Ink4a line, which can be grown in syngeneic immunocompetent FVB/NJ mice (18). Strikingly, mice orthotopically inoculated with shIRAK1+shIRAK4 KRas-Ink4a cells are completely healthy and showed no signs of distress for up to 6 months, whereas mice inoculated with shLacZ KRas-Ink4a cells all died by 40 days from large palpable tumors (Fig. 5F). On necropsy, none of the 10 pancreases inoculated with shIRAK1+shIRAK4 KRas-Ink4a cells showed any macro- or microscopic trace of tumor growth (not shown). This striking result again supports a critical role of IRAK in PDAC tumorigenesis. Next, we treated FVB/NJ mice with either vehicle, gemcitabine, IRAK1/4i, or both, 10 days after orthotopic inoculation with KRas-Ink4a cells. All mice were sacrificed when the vehicle-treated mice reached moribund status due to large palpable tumor or ascites. We found that mice treated with both gemcitabine and IRAK1/4i showed significantly reduced pancreatic tumor weight, compared with vehicle or gemcitabine-treated cohorts (Fig. 5G). Again, no mice showed any sign of toxicity or body weight loss during treatment (Supplementary Fig. S3A). Together, our data support testing IRAK4 inhibitor in combination with chemotherapy in PDAC treatment in clinical trials.

IRAK1/4i augments the cytotoxic effect of gemcitabine and suppresses tumor fibrosis

To study the *in vivo* effect of IRAK1/4i on PDAC, we analyzed tumors harvested from both the Capan-1 (Fig. 5D) and KRas-Ink4a (Fig. 5G) experiments. At lower magnifications, combo-treated tumors showed larger areas of necrosis compared with the other cohorts (Fig. 6A and Supplementary Fig. S3B). By multicolor IF, combo-treated tumors showed significantly less proliferative cells (double Ki-67$^+$, cytokeratin$^+$), higher apoptotic cells (cleaved-caspase-3$^+$; cytokeratin$^+$; Fig. 6A and Supplementary Fig. S3B), and less stromal fibroblasts (by α-SMA area) and fibrosis by trichrome staining (Fig. 6B and Supplementary Fig. S3B). Importantly, tumors treated with IRAK1/4i showed weaker, but not loss, of p-IRAK4 and p-TAK1 (a substrate of IRAK4) staining, compared with vehicle- or gemcitabine-treated tumors (Fig. 6C), indicating on-target effect. However, this observation also explains why knockdown of IRAK1 and IRAK4, or knockout of IRAK4, was much more effective in blocking tumorigenesis, underscoring the need to develop more potent IRAK4 inhibitor for clinical testing in the future.

Discussion

Overcoming the pathogenic NF-κB signaling is an actively pursued therapeutic strategy in PDAC (5). In this study, we demonstrate that PDAC commonly activates NF-κB through the innate immune IRAK kinases. Notably, the presence of p-IRAK4 is strongly associated with a higher chance of relapse and poor overall prognosis. However, it should be pointed out that our analysis using surgical PDAC tumors is confined to patients with

Downloaded from http://aacrjournals.org/clincancerres/article-pdf/23/7/1748/2043674/1748.pdf by guest on 26 August 2022

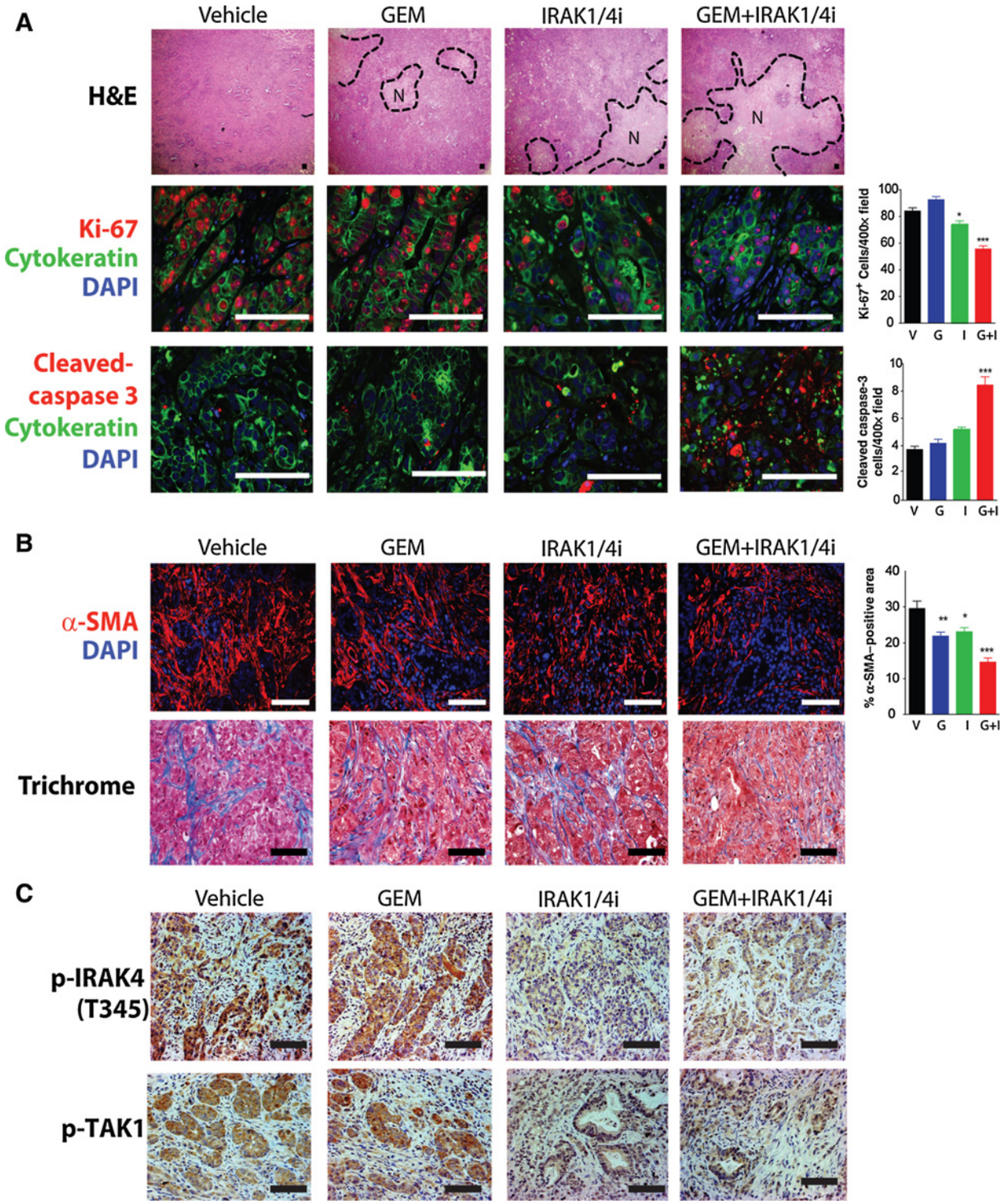

Figure 6.

IRAK1/4i cooperates with gemcitabine in inducing apoptosis, suppressing proliferation and fibrosis of PDAC tumor *in vivo*. **A,** Representative hematoxylin and eosin (H&E) and multicolor IF images of Capan-1 tumors treated as indicated. H&E staining showed large areas of necrosis (N) in tumors treated with both IRAK1/4 inhibitor and gemcitabine. Representative confocal IF images showing proliferation (Ki-67/red, cytokeratin/green, DAPI/blue) and apoptosis (cleaved-caspase-3/red, cytokeratin/green, DAPI/blue) of tumors in each treatment group. **B,** Representative images showing changes in α-SMA$^+$ area (CAFs/red, DAPI/blue) and fibrosis (blue) by trichrome staining. **C,** Representative IHC images of p-IRAK4 and p-TAK1 (a substrate of IRAK4) showing on-target effect of IRAK1/4i *in vivo*. Quantitative analyses were performed by analyzing multiple fields (8 tumors/group and 10 random 200X or 400X fields/tumor) using NIS-Elements software, and presented as mean ± SEM (*, $P < 0.05$; **, $P < 0.01$; ***, $P < 0.001$ by ANOVA; scale bar, 50 μm).

Downloaded from http://aacrjournals.org/clincancerres/article-pdf/23/7/1748/2043674/1748.pdf by guest on 26 August 2022

resectable disease, which represents only 10% to 15% of all PDAC cases (2). Patients with advanced or metastatic disease are routinely diagnosed with fine-needle aspiration, which does not allow for this kind of histologic study. Nonetheless, 80% of patients who underwent surgical resection eventually succumb to disease relapse despite adjuvant therapy (2), so identifying the mechanisms that affect patient survival is crucial for the development of effective adjuvant regimen to improve patient outcome. Herein, we provide proof of principle that suppression of IRAK4 can greatly cripple the growth of PDAC and augment the effect of chemotherapy *in vitro and in vivo*. However, in contrast to the dramatic effect of genetic ablation of IRAK4, the relatively modest antitumor effect of IRAK1/4i used in this study underscores the need to develop more potent IRAK4 inhibitors for clinical testing.

Aside from enhancing the survival of PDAC cells, IRAK4 appears to be a master regulator of a multitude of cytokines and chemokines including GM-CSF, CCL2, CXCL1, CXCL2, IL8, and IL-β, which are all known to modulate the intensely fibrotic and immune-suppressive TME of PDAC. For instance, PDAC-derived GM-CSF promotes recruitment of $Gr1^+CD11b^+$ myeloid cells, which inhibits $CD8^+$ T cells (36). The abundance of CCL2 in the PDAC microenvironment engages CCR2 receptor on tumor-associated macrophages to suppress $CD8^+$ cells and enhances tumor-initiating stem cells (18, 37). As such, addition of CCR2 inhibitor to chemotherapy FOLFIRINOX achieved an objective response of 49% in patients with metastatic PDAC (38). Necroptosis-induced CXCL1 secretion fuels PDAC progression by promoting macrophage-induced immune suppression (39). In an elegant study by Ling and colleagues (7), expression of oncogenic *KRas* activates NF-κB through enhanced secretion of IL1α. Although we did observe increased expression of IL1α following expression of $KRas^{G12D}$ in HPNE and HPDE cells, as published (7), we failed to detect upregulation of p-IRAK4 compared with vector control cells (not shown), indicating that the expression of oncogenic *KRas*, at least in cell culture model, is insufficient to induce IRAK4 phosphorylation. Therefore, further work using genetically engineered mouse models is warranted to clearly establish the signaling interplay between oncogenic *KRas* and the IRAK-IKK-NF-κB cascades in PDAC development.

Aside from PDAC, targeting the IRAK1/4 cascade has been shown to be a promising strategy in other malignancies including DLBCL (29, 40), myelodysplastic syndrome (41), T-cell ALL (42), melanoma (27), breast cancer (43), and head and neck cancer (44), further underscoring the urgent need to develop potent IRAK inhibitors for clinical testing. Another study showed that TAK1 inhibition could augment the effect of chemotherapy in PDAC (45). Supporting this study, we found that treatment of PDAC lines with TAK1 inhibitor 5Z-7-oxozeaenol significantly reduced AI growth and p-NF-κB/p65 (not shown), and that IRAK1/4i significantly reduced p-TAK1 (Fig. 6C and not shown).

How IRAK4 is activated in PDAC is currently unknown. Because activating mutations of IRAK4 or MyD88, the adaptor protein upstream of IRAK4, are not reported in PDAC from analysis of TCGA, COSMIC database and from our own Sanger sequencing of PDAC lines (not shown), we hypothesize that IRAK4 is activated by engagement of the interleukin receptors or the TLRs by pathogen- or damage-associated molecular patterns in the TME. To test this, we are currently conducting loss-of-function analysis of individual TLRs, as well as IL1R and IL18R, in multiple PDAC cells.

In summary, our study provides a strong rationale for targeting IRAK4 as a novel therapeutic approach in PDAC. We showed that p-IRAK4 is not only a strong prognostic marker for poor outcomes in patients with PDAC, but also a major driver of NF-κB activity and could be therapeutically exploited to improve chemotherapy response. Our work also suggests the need to develop and test more potent IRAK4 inhibitors in combination with chemotherapy in preclinical models. Furthermore, understanding how the IRAKs are activated in PDAC, using cell line and genetically engineered mouse models, will add invaluable knowledge to the biology of PDAC.

Disclosure of Potential Conflicts of Interest

No potential conflicts of interest were disclosed.

Disclaimer

The content is solely the responsibility of the authors and does not necessarily represent the official view of the NIH.

Authors' Contributions

Conception and design: D. Zhang, D.G. DeNardo, K.-H. Lim
Development of methodology: D. Zhang, L. Li, M.B. Ruzinova, K.-H. Lim
Acquisition of data (provided animals, acquired and managed patients, provided facilities, etc.): L. Li, H. Jiang, B. Knolhoff, M.B. Ruzinova, K.-H. Lim
Analysis and interpretation of data (e.g., statistical analysis, biostatistics, computational analysis): D. Zhang, L. Li, A. Wang-Gillam, M.B. Ruzinova, K.-H. Lim
Writing, review, and/or revision of the manuscript: A.C. Lockhart, A. Wang-Gillam, D.G. DeNardo, M.B. Ruzinova, K.-H. Lim
Administrative, technical, or material support (i.e., reporting or organizing data, constructing databases): D. Zhang, K.-H. Lim
Study supervision: K.-H. Lim

Acknowledgments

We wish to thank Dr. Ron Bose and Jeff Guo for critical reading of the article, Maureen K. Highkin for technical advice, Julie Prior at the Molecular Imaging Center (funded under P50 CA094056 from the NCI) for assistance with animal imaging and analysis, and the Digestive Disease Research Core Center (funded by grant P30DK052574 from the NIDDK) for providing technical support.

Grant Support

This study was supported by the NCI Cancer Center Support Grant # P30 CA091842 (K.-H. Lim), Washington University Institute of Clinical and Translational Sciences grant UL1 TR000448 from the NCATS of the NIH (K.-H. Lim), and Elsa Pardee Foundation Award (K.-H. Lim and M.B. Ruzinova).

The costs of publication of this article were defrayed in part by the payment of page charges. This article must therefore be hereby marked *advertisement* in accordance with 18 U.S.C. Section 1734 solely to indicate this fact.

Received May 3, 2016; revised September 19, 2016; accepted September 28, 2016; published OnlineFirst October 4, 2016.

References

1. Ryan DP, Hong TS, Bardeesy N. Pancreatic adenocarcinoma. N Engl J Med 2014;371:2140–1.
2. Siegel RL, Miller KD, Jemal A. Cancer statistics, 2016. CA Cancer J Clin 2016;66:7–30

Downloaded from http://aacrjournals.org/clincancerres/article-pdf/23/7/1748/2043674/1748.pdf by guest on 26 August 2022

3. Wang W, Abbruzzese JL, Evans DB, Larry L, Cleary KR, Chiao PJ. The nuclear factor-kappa B RelA transcription factor is constitutively activated in human pancreatic adenocarcinoma cells. Clin Cancer Res 1999;5:119–27.
4. Weichert W, Boehm M, Gekeler V, Bahra M, Langrehr J, Neuhaus P, et al. High expression of RelA/p65 is associated with activation of nuclear factor-kappaB-dependent signaling in pancreatic cancer and marks a patient population with poor prognosis. Br J Cancer 2007;97:523–30.
5. Carbone C, Melisi D. NF-kappaB as a target for pancreatic cancer therapy. Expert Opin Ther Targets 2012;16Suppl 2:S1–10.
6. Prabhu L, Mundade R, Korc M, Loehrer PJ, Lu T. Critical role of NF-kappaB in pancreatic cancer. Oncotarget 2014;5:10969–75.
7. Ling J, Kang Y, Zhao R, Xia Q, Lee DF, Chang Z, et al. KrasG12D-induced IKK2/beta/NF-kappaB activation by IL-1alpha and p62 feedforward loops is required for development of pancreatic ductal adenocarcinoma. Cancer Cell 2012;21:105–20.
8. Bang D, Wilson W, Ryan M, Yeh JJ, Baldwin AS. GSK-3alpha promotes oncogenic KRAS function in pancreatic cancer via TAK1-TAB stabilization and regulation of noncanonical NF-kappaB. Cancer Discov 2013;3:690–703.
9. Lu Z, Li Y, Takwi A, Li B, Zhang J, Conklin DJ, et al. miR-301a as an NF-kappaB activator in pancreatic cancer cells. EMBO J 2011;30:57–67.
10. Bournazou E, Bromberg J. Targeting the tumor microenvironment: JAK-STAT3 signaling. JAKSTAT 2013;2:e23828.
11. Feig C, Gopinathan A, Neesse A, Chan DS, Cook N, Tuveson DA. The pancreas cancer microenvironment. Clin Cancer Res 2012;18:4266–76.
12. Lim KH, Staudt LM. Toll-like receptor signaling. Cold Spring Harb Perspect Biol 2013;5.
13. Ikebe M, Kitaura Y, Nakamura M, Tanaka H, Yamasaki A, Nagai S, et al. Lipopolysaccharide (LPS) increases the invasive ability of pancreatic cancer cells through the TLR4/MyD88 signaling pathway. J Surg Oncol 2009;100:725–31.
14. Ochi A, Graffeo CS, Zambirinis CP, Rehman A, Hackman M, Fallon N, et al. Toll-like receptor 7 regulates pancreatic carcinogenesis in mice and humans. J Clin Invest 2012;122:4118–29.
15. Zambirinis CP, Levie E, Nguy S, Avanzi A, Barilla R, Xu Y, et al. TLR9 ligation in pancreatic stellate cells promotes tumorigenesis. J Exp Med 2015;212:2077–94.
16. Kim TW, Staschke K, Bulek K, Yao J, Peters K, Oh KH, et al. A critical role for IRAK4 kinase activity in Toll-like receptor-mediated innate immunity. J Exp Med 2007;204:1025–36.
17. Li S, Strelow A, Fontana EJ, Wesche H. IRAK-4: A novel member of the IRAK family with the properties of an IRAK-kinase. Proc Natl Acad Sci U S A 2002;99:5567–72.
18. Mitchem JB, Brennan DJ, Knolhoff BL, Belt BA, Zhu Y, Sanford DE, et al. Targeting tumor-infiltrating macrophages decreases tumor-initiating cells, relieves immunosuppression, and improves chemotherapeutic responses. Cancer Res 2013;73:1128–41.
19. Hayes TK, Neel NF, Hu C, Gautam P, Chenard M, Long B, et al. Long-term ERK inhibition in KRAS-mutant pancreatic cancer is associated with MYC degradation and senescence-like growth suppression. Cancer Cell 2016;29:75–89.
20. Jones S, Zhang X, Parsons DW, Lin JC, Leary RJ, Angenendt P, et al. Core signaling pathways in human pancreatic cancers revealed by global genomic analyses. Science 2008;321:1801–6.
21. Bachem MG, Schneider E, Gross H, Weidenbach H, Schmid RM, Menke A, et al. Identification, culture, and characterization of pancreatic stellate cells in rats and humans. Gastroenterology 1998;115:421–32.
22. O'Hayer KM, Counter CM. A genetically defined normal somatic human cell system to study ras oncogenesis in vitro and in vivo. Methods Enzymol 2006;407:637–47.
23. Chou TC. Drug combination studies and their synergy quantification using the Chou-Talalay method. Cancer Res 2010;70:440–6.
24. Baines AT, Lim KH, Shields JM, Lambert JM, Counter CM, Der CJ, et al. Use of retrovirus expression of interfering RNA to determine the contribution of activated K-Ras and ras effector expression to human tumor cell growth. Methods Enzymol 2006;407:556–74.
25. Kawasaki T, Kawai T. Toll-like receptor signaling pathways. Front Immunol 2014;5:461.
26. Rhyasen GW, Starczynowski DT. IRAK signalling in cancer. Br J Cancer 2015;112:232–7.
27. Srivastava R, Geng D, Liu Y, Zheng L, Li Z, Joseph MA, et al. Augmentation of therapeutic responses in melanoma by inhibition of IRAK-1,-4. Cancer Res 2012;72:6209–16.
28. Powers JP, Li S, Jaen JC, Liu J, Walker NP, Wang Z, et al. Discovery and initial SAR of inhibitors of interleukin-1 receptor-associated kinase-4. Bioorg Med Chem Lett 2006;16:2842–5.
29. Ngo VN, Young RM, Schmitz R, Jhavar S, Xiao W, Lim KH, et al. Oncogenically active MYD88 mutations in human lymphoma. Nature 2011;470:115–9.
30. Fraczek J, Kim TW, Xiao H, Yao J, Wen Q, Li Y, et al. The kinase activity of IL-1 receptor-associated kinase 4 is required for interleukin-1 receptor/toll-like receptor-induced TAK1-dependent NFkappaB activation. J Biol Chem 2008;283:31697–705.
31. Koziczak-Holbro M, Joyce C, Gluck A, Kinzel B, Muller M, Tschopp C, et al. IRAK-4 kinase activity is required for interleukin-1 (IL-1) receptor- and toll-like receptor 7-mediated signaling and gene expression. J Biol Chem 2007;282:13552–60.
32. Arlt A, Gehrz A, Muerkoster S, Vorndamm J, Kruse ML, Folsch UR, et al. Role of NF-kappaB and Akt/PI3K in the resistance of pancreatic carcinoma cell lines against gemcitabine-induced cell death. Oncogene 2003;22:3243–51.
33. Tjomsland V, Spangeus A, Valila J, Sandstrom P, Borch K, Druid H, et al. Interleukin 1alpha sustains the expression of inflammatory factors in human pancreatic cancer microenvironment by targeting cancer-associated fibroblasts. Neoplasia 2011;13:664–75.
34. Mews P, Phillips P, Fahmy R, Korsten M, Pirola R, Wilson J, et al. Pancreatic stellate cells respond to inflammatory cytokines: Potential role in chronic pancreatitis. Gut 2002;50:535–41.
35. Vonlaufen A, Phillips PA, Xu Z, Goldstein D, Pirola RC, Wilson JS, et al. Pancreatic stellate cells and pancreatic cancer cells: An unholy alliance. Cancer Res 2008;68:7707–10.
36. Pylayeva-Gupta Y, Lee KE, Hajdu CH, Miller G, Bar-Sagi D. Oncogenic Kras-induced GM-CSF production promotes the development of pancreatic neoplasia. Cancer Cell 2012;21:836–47.
37. Sanford DE, Belt BA, Panni RZ, Mayer A, Deshpande AD, Carpenter D, et al. Inflammatory monocyte mobilization decreases patient survival in pancreatic cancer: A role for targeting the CCL2/CCR2 axis. Clin Cancer Res 2013;19:3404–15.
38. Nywening TM, Wang-Gillam A, Sanford DE, Belt BA, Panni RZ, Cusworth BM, et al. Targeting tumour-associated macrophages with CCR2 inhibition in combination with FOLFIRINOX in patients with borderline resectable and locally advanced pancreatic cancer: A single-centre, open-label, dose-finding, non-randomised, phase 1b trial. Lancet Oncol 2016;17:651–62.
39. Seifert L, Werba G, Tiwari S, Giao Ly NN, Alothman S, Alqunaibit D, et al. The necrosome promotes pancreatic oncogenesis via CXCL1 and Mincle-induced immune suppression. Nature 2016;532:245–9.
40. Kelly PN, Romero DL, Yang Y, Shaffer AL3rd, Chaudhary D, Robinson S, et al. Selective interleukin-1 receptor-associated kinase 4 inhibitors for the treatment of autoimmune disorders and lymphoid malignancy. J Exp Med 2015;212:2189–201.
41. Rhyasen GW, Bolanos L, Fang J, Jerez A, Wunderlich M, Rigolino C, et al. Targeting IRAK1 as a therapeutic approach for myelodysplastic syndrome. Cancer Cell 2013;24:90–104.
42. Li Z, Younger K, Gartenhaus R, Joseph AM, Hu F, Baer MR, et al. Inhibition of IRAK1/4 sensitizes T cell acute lymphoblastic leukemia to chemotherapies. J Clin Invest 2015;125:1081–97.
43. Wee ZN, Yatim SM, Kohlbauer VK, Feng M, Goh JY, Bao Y, et al. IRAK1 is a therapeutic target that drives breast cancer metastasis and resistance to paclitaxel. Nat Commun 2015;6:8746.
44. Adams AK, Bolanos LC, Dexheimer PJ, Karns RA, Aronow BJ, Komurov K, et al. IRAK1 is a novel DEK transcriptional target and is essential for head and neck cancer cell survival. Oncotarget 2015;6:43395–407.
45. Melisi D, Xia Q, Paradiso G, Ling J, Moccia T, Carbone C, et al. Modulation of pancreatic cancer chemoresistance by inhibition of TAK1. J Natl Cancer Inst 2011;103:1190–204.

Downloaded from http://aacrjournals.org/clincancerres/article-pdf/23/7/1748/2043674/1748.pdf by guest on 26 August 2022